



HAL
open science

Experimental study of gas diffusion in cement paste

J. Sercombe, R. Vidal, C. Galle, F. Adenot

► **To cite this version:**

J. Sercombe, R. Vidal, C. Galle, F. Adenot. Experimental study of gas diffusion in cement paste. Cement and Concrete Research, 2006, 37 (4), pp.579-588. 10.1016/j.cemconres.2006.12.003 . cea-02360113

HAL Id: cea-02360113

<https://cea.hal.science/cea-02360113>

Submitted on 20 Nov 2019

HAL is a multi-disciplinary open access archive for the deposit and dissemination of scientific research documents, whether they are published or not. The documents may come from teaching and research institutions in France or abroad, or from public or private research centers.

L'archive ouverte pluridisciplinaire **HAL**, est destinée au dépôt et à la diffusion de documents scientifiques de niveau recherche, publiés ou non, émanant des établissements d'enseignement et de recherche français ou étrangers, des laboratoires publics ou privés.

Correspondence

Dr. SERCOMBE Jérôme
CEA CADARACHE
DEN/DEC/SESC/LSC - Bât. 151
13108 Saint-Paul-Lez-Durance
FRANCE
Tel : 33-4-42-25-30-72
Fax : 33-4-42-25-29-49
E-mail-address : sercombe@cea.fr

Paper Title :

Experimental study of gas diffusion in cement paste

Authors : Jérôme Sercombe*, Romain Vidal, Christophe Gallé, Frédéric Adenot

Key words : Humidity (A), Microstructure (B), Diffusion (C), Transport properties (C), Cement paste (D), Hydrogen.

Experimental study of gas diffusion in cement paste

J. Sercombe^a, R. Vidal^b, C. Gall c, F. Adenot^d,

Abstract

This paper presents an experimental study of gas diffusion (hydrogen, nitrogen and xenon) through cement pastes (CEM I and CEM V) of different water/cement ratios (0.35 and 0.45). First, the impact of Relative Humidity (RH) on gas diffusion is investigated by performing tests on samples pre-conditioned in specific atmospheric conditions (dry, 55, 70, 82, 93 and 100% RH) by means of saline solutions. The comparison of the results obtained for the CEM I and the CEM V samples (w/c ratio of 0.45) demonstrate the importance of pore size distribution/connectivity on gas diffusion. Second, diffusion tests at different total pressures and using two different mixtures (hydrogen-nitrogen, xenon-nitrogen) are performed to study the nature of gas diffusion in cement paste. Results demonstrate that gas diffusion in cement paste is controlled by Knudsen diffusion rather than by ordinary diffusion.

^a D.Sc., Res. Eng., Atomic Energy Commission, Cadarache, 13108 Saint-Paul-Lez-Durance, France.

^b Res. Eng., Atomic Energy Commission, Cadarache, 13108 Saint-Paul-Lez-Durance, France.

^c D.Sc., Laboratory Head, Atomic Energy Commission, Saclay, 91191 Gif-sur-Yvette, France.

^d D.Sc., Laboratory Head, Atomic Energy Commission, Cadarache, 13108 Saint-Paul-Lez-Durance, France.

Introduction

Durability of concrete structures often depends on the rate of ingress of gaseous or aqueous elements into the concrete porous network. Migration of gaseous elements in concrete can be driven by pressure or concentration gradients, i.e., by viscous flow or diffusion. Carbonation is a typical example where gas diffusion, i.e., carbon dioxide, plays an important role with respect to the overall kinetics of the deterioration process [1, 2, 3]. Drying is another example where the kinetics of gas diffusion, i.e., vapour water diffusion, can be of some importance [4, 5, 6]. In consequence, many mathematical descriptions used to estimate the durability of concrete structures depend on the diffusion coefficient of gas species in the porous network of concrete.

Gas diffusion through porous media is often divided in three independent modes or mechanisms with a distinct diffusion coefficient for each of them [7]: free-molecule or Knudsen diffusion, molecular or ordinary diffusion and surface diffusion. Usually surface diffusion is neglected, mostly because it is basically an assumption which does not rest on experimental evidence. Theoretically, ordinary diffusion, in which the different species of a mixture move relative to each other under the influence of concentration gradients, occurs predominantly when molecule-molecule collisions dominate over molecule-pore wall collisions. On the contrary, Knudsen diffusion, in which molecules of different species move entirely independently of each other, occurs predominantly when molecule-molecule collisions can be ignored compared to molecule-pore wall collisions.

The prevalence of Knudsen or ordinary diffusion depends, first, on the mean free

path of the gas molecule (approximately $0.1 \mu\text{m}$ for a gas molecule at atmospheric pressure and 20°C) which depends itself on the total pressure, the temperature of the gas mixture and on the molecular weight of the gas species, second, on the size (diameter if the pores are assumed to be cylindrical) and degree of connectivity of the unsaturated pores (accessible to gas). Since the pore diameters in cement pastes, mortars or concretes are widely distributed from the nanometer to the millimeter scale, it is difficult to state, a priori, which is the dominant mechanism in cementitious materials.

Furthermore, the pore size distribution and degree of connectivity of the unsaturated pores in cementitious materials strongly rely on the mix-design properties (w/c ratio, type of cement, proportion of aggregates,...) and on the curing/conservation conditions (Relative Humidity, temperature) which modify the moisture content and saturation level (i.e., the percentage of the total pore volume filled with water) of the materials. In this respect, some studies have pointed out the importance of moisture content, w/c ratio, aggregate content, type of cement, curing/conservation conditions on the diffusion of gas through mortars or concretes [8, 9, 10, 11].

To the authors knowledge, the prevalence of Knudsen or ordinary diffusion in cementitious materials has never been assessed clearly in spite of its importance with respect to the mathematical description of diffusion-based phenomena (carbonation, drying, ...). In this paper, the impact of the moisture content, the total porosity and pore size distribution, of the total gas pressure and of the gas molecular weight on gas diffusion in pure cement pastes is therefore investigated experimentally. Con-

clusions are then given concerning the prevalence of Knudsen or ordinary diffusion at low to moderate pressures.

1. Modes of gas transport in porous media

Usually, four modes of gas transport can be considered in porous media [7], as illustrated schematically in Figure (1). Three of them are related to concentration or partial pressure gradients (ordinary diffusion, Knudsen diffusion, surface diffusion), and one to the total gas pressure gradient (viscous or bulk flow). In the discussion which follows, no total pressure gradient (no bulk flow) is considered since this is the condition which prevails in the experiments presented in this paper. Surface diffusion is neglected since its contribution to the overall transport cannot be assessed precisely. Binary gas mixtures only are considered.

1.1. Molecular or ordinary diffusion

Molecular diffusion defines the mechanism by which the different species of a mixture move relative to each other under the influence of concentration gradients, and where molecule-molecule collisions dominate over molecule-pore wall collisions, see Figure (1). This case is encountered when the mean free path λ of gas molecules (the mean free path of a gas molecule at atmospheric pressure is approximately $0.1 \mu\text{m}$) is much smaller than the characteristic length scale of the pores (the pore diameter if the pores are assumed to be cylindrical). For a binary mixture, in which there is no pressure gradient, the purely diffusive fluxes J_{1D} and J_{2D} in a porous material can

be written as :

$$J_{1D} = -D_{12}\nabla c_1 \quad (1)$$

$$J_{2D} = -D_{21}\nabla c_2 \quad (2)$$

where D_{12} and D_{21} are the gas diffusion coefficients, ∇c_1 and ∇c_2 the concentration gradients of gas species 1 and 2 in the pore volume, such that $D_{12} = D_{21}$ and $\nabla c_1 + \nabla c_2 = 0$. The measurable binary gas diffusion coefficients D_{12} and D_{21} through the porous medium are usually related to the free gas diffusion coefficient $D_{12}^{free} = D_{21}^{free}$ of the gas species in open space as follows [7] :

$$D_{ij} = \frac{\epsilon_g}{\tau} D_{ij}^{free} \quad (3)$$

where ϵ_g and τ are respectively the percentage of open pores in which ordinary diffusion can take place (unsaturated and interconnected pores) and the tortuosity, i.e., the average length of the diffusion path in the material. Complex relations based on pore geometrical arguments have been derived for the tortuosity factor, which usually depends on the total porosity and the saturation level of the porous medium [13, 14].

The free gas diffusion coefficient D_{12}^{free} in a binary gas mixture at low to moderate pressures is well known and results from the molecular theory of gases. The following approximate expression can be obtained in many textbook on the subject [16, 17]:

$$D_{12}^{free} = 1.858 \times 10^{-7} \left(\frac{1}{M_1} + \frac{1}{M_2} \right)^{1/2} \frac{T^{3/2}}{P\sigma_{12}^2\Omega_D} \quad (4)$$

with T the absolute temperature (K), P the pressure of the gas mixture (bars), M_i the molecular weight of gas i (g/mol), σ_{12} the characteristic length (Å) and Ω_D ,

the diffusion collision integral (-). Ω_D can be estimated according to the formulae given in the appendix. Expression (4) shows that the free gas diffusion coefficient in a binary mixture is inversely proportional to the pressure of the gas mixture, i.e., $D_{12}^{free} = f(1/P)$. According to eq. (3), a similar dependency can be expected for the diffusion coefficient D_{ij} through the porous medium in case ordinary diffusion is predominant.

1.2. Free- or Knudsen diffusion

In the free-molecule or Knudsen diffusion mechanism, the gas molecules collide more frequently with the pore walls than with other gas molecules, see Figure (1). This case is encountered when the mean free path λ of the gas molecules is of the order of the characteristic length scale of the pores (diameter D if cylindrical). Since molecule-molecule interactions are negligible, the Knudsen diffusion flux J_{iD} is independent of the gas composition and is therefore defined for each gas species i by the following relation [7] :

$$J_{iK} = -D_{iK} \nabla c_i \quad (5)$$

with D_{iK} as the Knudsen diffusion coefficient of gas species i in the porous medium, ∇c_i the concentration gradient of gas species i . Due to the complexity of the geometry of most porous network, attempts have been made to related the macroscopic Knudsen diffusion coefficient D_{iK} to that of a single cylindrical pore of average radius r (mean radius of the pores in which diffusion can take place, assumed cylindrical

and interconnected) through a relation similar to eq. (3) :

$$D_{iK} = \frac{\epsilon_g}{\tau} D_{iK}^{pore} \quad (6)$$

with D_{iK}^{pore} the Knudsen diffusion coefficient through a single pore of radius r and ϵ_g/τ the porosity/tortuosity factor as previously defined. For a long cylindrical pore, D_{iK}^{pore} can be expressed as follows in function of the mean pore radius r and the gas species molecular weight M_i [7, 13]:

$$D_{iK}^{pore} = \frac{2r}{3} \sqrt{\frac{8RT}{\pi M_i}} \quad (7)$$

Note that D_{iK}^{pore} is independent of the pressure of the gas mixture and inversely proportional to $\sqrt{M_i}$. According to eq. (6), this should also be the case for the Knudsen diffusion coefficient D_{iK} of gas species i in the porous medium.

1.3. Combination of diffusion mechanisms for binary mixtures

The combination of ordinary and Knudsen diffusion for a binary mixture of gas species i and j is based on momentum-transfer arguments [7]. According to Newton's second law of motion, if a gas species i is not accelerated on the average, then the momentum transferred to it by collisions with the walls and with species j must be balanced by the external force acting on it, i.e., the gradient of the partial pressure of the species i , ∇p_i . Equations (1) and (5) might be rewritten as follows :

$$(\nabla p_i)_{molecule} = \frac{RT}{D_{ij}} J_{iD} \quad (8)$$

$$(\nabla p_i)_{wall} = \frac{RT}{D_{iK}} J_{iK} \quad (9)$$

Combining (8) and (9) with the equilibrium condition $\nabla p_i = (\nabla p_i)_{molecule} + (\nabla p_i)_{wall}$, the following expression for the combined Knudsen-ordinary diffusion of one component i of a binary mixture at uniform total pressure is obtained :

$$(\nabla p_i) = \frac{RT}{D_{ij}} J_{iD} + \frac{RT}{D_{iK}} J_{iK} \quad (10)$$

From eq. (10), the total flux of species i , $J_i = J_{iD} + J_{iK}$ can now be written as :

$$J_i = -D_i \nabla c_i \quad (11)$$

with the combined Knudsen-ordinary diffusion coefficient D_i of species i in the porous material given by :

$$D_i = \left(\frac{1}{D_{iK}} + \frac{1}{D_{ij}} \right)^{-1} = \frac{\epsilon_g}{\tau} \left(\frac{1}{D_{iK}^{pore}} + \frac{1}{D_{ij}^{free}} \right)^{-1} \quad (12)$$

Relation (12) refers to a parallel model, as indicated in reference [13]. It differs from the approach adopted by Klinkenberg [15] to combine Knudsen diffusion and viscous flow [12] (serie model). It is of some interest to note that, according to the above-mentioned pressure dependency of D_{iK}^{pore} and D_{ij}^{free} , the combined Knudsen-ordinary diffusion coefficient D_i tends towards the Knudsen diffusion coefficient D_{iK} when the total pressure of the binary gas mixture tends towards 0. This is consistent with the fact that the mean free path tends to infinity when pressure drops to zero. The mean free path becomes therefore much greater than the characteristic size of the pores. Molecule-pore wall collisions are thus predominant.

2. Experimental program

2.1. Materials: characteristics, conditioning and sampling

The experimental program has been carried out on hardened cement pastes made of French industrial CEM I (OPC) and CEM V (BFS-PFA) cements. Cement pastes were preferred to concretes or mortars since diffusion tests could be performed on relatively thin specimen (20 mm) which can be considered homogeneous. Six cylindrical probes (40 mm diameter and 80 mm high) per cement type (CEM I and V) and w/c ratio (0.35 and 0.45) have been prepared in 1994. After demoulding, they have been cured at 20°C for 9 months in a $Ca(OH)_2$ water saturated solution. After this period, they were kept for almost 10 years in sealed dessicators where the Relative Humidity (RH) was controlled by saturated salt solutions, as indicated in Table 1. To study the diffusion properties of the "dry" materials, one probe of each hardened cement paste was also kept in sealed dessicators containing silica gel (RH \approx 3%). In 2003, the central part of the probes were cut in 20 mm thick slices, three per probe. The end parts of the probes, 10 mm thick, were also kept in order to estimate the total porosity and the density of the cement pastes. The porosity has been measured by complete drying at 60°C and re-saturation of the samples at atmospheric pressure. The main physical properties of the studied cement pastes are given in Table (2). After the sawing operation and before testing, the 10 and 20 mm thick samples have been re-conditioned in the same atmospheric conditions as before sawing.

2.2. Experimental setup

The main element of the experimental set-up is the diffusion cell, as shown in Fig. (2). It consists of two stainless steel compartments of equal dimensions (internal diameter 60 mm, internal length 90 mm, total volume of about 90 ml), separated by the cement paste sample, glued with an epoxy to two half stainless steel rings. The ring system is designed to ensure the gas tightness on the outer surface of the cement paste sample. To this end, it covers partly the flat faces of the cement paste samples, leaving a diffusion surface of 20 mm in diameter, see Fig. (2). The airtightness of the cell is ensured by rubber O-rings which are in contact with the two steel rings.

The experimental set-up used for the diffusion tests, as sketched in Fig. (3), consists of a diffusion cell, vacuum pumps, pressure sensors, gas flow lines and a chromatograph. The vacuum pumps are used at the beginning of the test to eliminate the gas phase initially in the diffusion cell and in the gas flow lines. The pressure sensors are used to control and monitor during the test the pressure of the gas mixture in the two compartments of the diffusion cell. The chromatograph is used to analyze periodically the gas mixture in one of the two compartments.

A diffusion test comprises the following steps. The vacuum is first made in the two compartments of the diffusion cell and in the gas flow lines. One compartment is then filled with pure hydrogen or xenon, the other with pure nitrogen. Periodic analyses of the gas mixture in the nitrogen compartment are then realized. Since an analysis results in a small gas expansion due to the non-negligible volume of the

gas flow lines situated between the nitrogen compartment and the chromatograph, the nitrogen compartment is immediately re-filled with pure nitrogen after each measure. This ensures that the gas pressure in the two compartments remains equal during the test. Gas analyses are performed till the steady diffusion state is reached. The duration of a diffusion test depends on the initial water content of the cement paste sample. For saturated samples, it can last several months. For dry samples, the steady state is usually reached within a few minutes. The mass of the samples are measured before and after each diffusion test in order to check the constancy of the cement paste water content.

Two VARIAN 3400 chromatographs are used for the gas analyses : one with argon as the carrier gas (for the nitrogen-hydrogen gas mixture) and one with helium (for the nitrogen-xenon gas mixture). The change in carrier gas is made to increase the sensitivity of the measures. A molecular sieve is used to remove moisture from the gas mixtures before passing through the capillary columns of the chromatographs for separation. The operating temperature of the chromatographic ovens is of 180°C, which allows to perform analyses in less than 10 minutes. The chromatographs use thermal conductivity detectors to identify and quantify the elements of the gas mixture. Since the identification is not limited to nitrogen, hydrogen and xenon, any lack of air tightness in the diffusion cell is immediately seen through the detection of small quantities of oxygen. For the gas species of interest (hydrogen, xenon), a precise calibration of the thermal conductivity detectors is made prior to the tests which allows for the quantification of very small percentage in the gas mixture (as

low as 0.01 %).

3.3. Measurement of the diffusion coefficient

Gas analyses in the nitrogen compartment are performed regularly till the steady diffusive flow is obtained. The analyses give access to the evolution in time of the quantity of hydrogen (or xenon) that has passed through the cement paste sample, $Q_i(t)$ with $i = H_2$ or Xe . Considering one-dimensional diffusion through a cement paste sample of thickness L , and using the steady-state assumption, equation (11) for the total diffusive flux of a gas species i can be re-cast as follows :

$$J_i = -D_i \frac{c_i^u(t) - c_i^d(t)}{L} \quad (13)$$

with $c_i^u(t)$ and $c_i^d(t)$ respectively as the concentration of gas species i in the upstream and downstream compartments of the diffusion cell. At the beginning of the diffusion test, the upstream compartment is filled with the gas species i (H_2 or Xe), and hence $c_i^u(t = 0) = c_i^\circ$. The downstream compartment is filled with nitrogen and hence $c_i^d(t = 0) = 0$. The test is then performed till steady state is reached. This is usually achieved for small concentrations of gas species i (less than 5%) in the downstream compartment of the diffusion cell. Hence the change in concentration gradient during the test can be neglected :

$$c_i^u(t) - c_i^d(t) \approx c_i^u(t = 0) - c_i^d(t = 0) = c_i^\circ \quad (14)$$

Integration in time of equation (13) with the condition (14) leads to the following expression for the quantity of gas species i that has passed through the cement paste

sample :

$$Q_i(t) = \frac{Sc_i^\circ}{L}D_it \quad (15)$$

with S the surface of cement paste available to gas diffusion. By plotting $Q_i \times L/S/c_i^\circ$ in function of time as obtained from the periodic gas analyses, it is then possible to estimate the combined Knudsen-ordinary diffusion coefficient D_i , as shown in Figure (4). Linear regression is used to best-fit the experimental data. Only the last 5 – 6 points are used since the first measures are characteristic of the transient regime. This method is valid only for gases which are inert with respect to the cement paste. This is the case of hydrogen, xenon, and nitrogen.

4. Experimental results and discussion

4.1. Impact of w/c ratio and cement type on hydrogen diffusion

All the diffusion tests presented hereafter have been performed with a hydrogen-nitrogen gas mixture at a total pressure of 1 bar. The mean hydrogen diffusion coefficients measured on the three cement pastes (CEM I with w/c ratios equal to 0.35 and 0.45, CEM V with a w/c ratio equal to 0.45) pre-conditioned in specific atmospheric conditions (3, 55, 70, 82, 93 and 100% RH) are given in Table (3). In general, three measures per cement type and hygral condition (RH) have been made. The results show the pronounced evolution of the diffusion coefficient with the moisture content of the samples.

To get a better picture of this evolution, the hydrogen diffusion coefficients of the two CEM I cement pastes are plotted in Figure (5) in function of the RH. The continuous

lines of Figure (5) join the mean diffusion coefficients obtained for each cement paste and hygral condition (RH). The shape of the curves obtained for the two cement pastes are similar. First, they present a plateau for RHs between 0 and 55% (mean diffusion coefficient of about 10^{-6} m²/s). The plateau is followed by a considerable decrease of the diffusion coefficient till 82%-93% RH (mean value of about 10^{-10} m²/s). The measures obtained on fully saturated samples (RH 100%) indicate that the diffusion coefficient decreases again when the RH exceeds 93%, leading values between 10^{-11} and 10^{-13} m²/s. A higher discrepancy in the experimental results has been observed for samples kept at high RHs (82–100%). This higher discrepancy results probably from the increasing importance of any heterogeneity on diffusion when the pore network is close to full saturation.

The porosity of OPC pastes (CEM I) can usually be split up in two major components : 1) the capillary porosity (pore diameters in the 3 – 100 nm range), which depends strongly on the w/c ratio and 2) the microporosity, associated with the C-S-H gel. The C-S-H gel porosity, being closely related to the C-S-H internal structure, is known to vary little with the w/c ratio [19, 18]. According to water vapour desorption test results [19], the capillary porosity is first desaturated when the RH decreases from 100% till 40-50%. For lower RHs, it is essentially the micropores which are desaturated [19, 18]. As shown by the curves of Figure (5), the impact of the w/c ratio on diffusion appears to be particularly important for RHs greater than 55% : in this domain, the diffusion coefficient of the CEM I, w/c=0.45 cement paste, is 2 to 8 times greater than that of the CEM I, w/c=0.35 cement paste. This

difference can be attributed to the increase of the capillary porosity with the w/c ratio. On the contrary, the w/c ratio has a very limited impact on diffusion when the RH is less than 55%, see Figure (5). This result is consistent with the fact that it is mainly the C-S-H pores which are water-desaturated at low RHs.

Surprisingly, the desaturation of C-S-H pores, which represent a considerable part of the total porosity (usually around 50%), does not lead to an increase of hydrogen diffusivity in the cement paste, as shown by the plateau obtained for RHs in the range 3-55%, see Figure (5). This result can possibly be explained by the small size of the C-S-H pores (1 – 3 nanometers in diameter) which may make them improper to gas diffusion, or by the important porous network that is already available to gas diffusion as a result of the desaturation of capillary pores.

The impact of the pore size distribution on hydrogen diffusion can further be stretched by plotting the results obtained for the CEM I (OPC) and CEM V (BFS-PFA) cement paste samples. It should be recalled that, in spite of their relatively close total porosities (see Table 2), the pore spaces of the two cement pastes are known, according to microstructural studies, permeability tests [20, 21], and radionuclides diffusion tests [22], to be very different. In particular, MIP (Mercury Intrusion Porosimetry) test results show that the percolation threshold for CEM V cement pastes is found for much smaller pore access diameters than for CEM I cement pastes. This indicates that the pore connectivity of CEM V materials is not as good as in CEM I materials (increased tortuosity). In particular, the capillary porosity of mature CEM V cement pastes is usually thought to be markedly

discontinuous [23].

The hydrogen diffusion coefficients of the w/c 0.45 CEM I and CEM V cement pastes are plotted in Figure (6) in function of the RH. The continuous lines of Figure (6) join the mean diffusion coefficients obtained for each cement paste and hygral condition (RH). The shape of the two curves of Figure (6) are close but the diffusion coefficient drop in the case of the CEM V curve seems translated towards higher RHs. Both curves present a plateau for RHs between 3 and 55%. The mean hydrogen diffusion coefficients for the two materials are however very different at this stage, being close to 10^{-6} m²/s and 5.10^8 m²/s for the CEM I and CEM V cement pastes, respectively. The plateau is followed by a slow decrease of the diffusion coefficient till 70% RH for the CEM I material (mean value of 6.10^{-7} m²/s) and 82% RH for the CEM V (mean value of 4.10^{-9} m²/s). A rapid decrease of the diffusion coefficients over 3 orders of magnitude is then observed for both materials when the RH increases. The average diffusion coefficients obtained for the two cement pastes at 93% RH are finally very different, being equal to 4.10^{-10} m²/s for the CEM I and 3.10^{-12} m²/s for the CEM V. Measures made on saturated samples (100% RH) indicate a further decrease of the hydrogen diffusion coefficient in both materials. In particular, no hydrogen flow has been observed during two of the three 7-months long diffusion tests performed on CEM V saturated samples.

The impact of pore connectivity on gas diffusion in cement paste can probably best be seen by comparing the diffusion coefficients obtained on the dry CEM I and CEM V samples, see the 3% RH column in Table (3). The diffusion of hydrogen in the dry

CEM V cement paste is almost 20 times slower than in the dry CEM I cement paste. Since the evolution of the diffusion coefficients between the dry state and 55% RH is very small for both cement pastes (RH range where the micropores are desaturated), these results can be attributed to main differences in the capillary pore system of the two cement pastes. They are consistent with the expected discontinuity of capillary pores in the CEM V cement paste. They confirm that pore connectivity has a great impact on gas diffusion in cement pastes.

4.3. Impact of the gas molecular weight on gas diffusion in cement paste

To study the impact of the gas molecular weight on gas diffusion in cement pastes, diffusion tests have been performed on the CEM I w/c 0.45 cement paste samples with hydrogen-nitrogen and xenon-nitrogen gas mixtures. Xenon was selected first because of its high molecular weight (131 g/mol) as compared to hydrogen (2 g/mol) and second because of its inert nature. According to Eq. (4), the free diffusion coefficient of xenon in nitrogen at 1 bar is equal to $1.24 \cdot 10^{-5} \text{ m}^2/\text{s}$. That of hydrogen in nitrogen at the same pressure is equal to $7.53 \cdot 10^{-5} \text{ m}^2/\text{s}$ (see the appendix for the application of Eq. (4) to hydrogen-nitrogen and xenon-nitrogen gas mixtures). In theory, if ordinary diffusion predominates and if the porosity/tortuosity factor is the same for xenon and hydrogen, then the hydrogen to xenon diffusion coefficient ratio in cement paste equals that of the same gas species in open space :

$$\frac{D_{Xe}}{D_{H_2}} = \frac{D_{Xe/N_2}^{free}}{D_{H_2/N_2}^{free}} = \frac{1.2410^{-5}}{7.5310^{-5}} = 0.165 \quad (16)$$

Applying in the same manner Eq. (7) and (8) to xenon and hydrogen, the hydrogen to xenon diffusion coefficient ratio in cement paste, in case Knudsen diffusion predominates, is given by :

$$\frac{D_{Xe}}{D_{H_2}} = \sqrt{\frac{M_{H_2}}{M_{Xe}}} = \sqrt{\frac{2}{131}} = 0.124 \quad (17)$$

Note that the diffusion coefficients ratios of Eqs. (16) and (17) are very close.

The diffusion tests have been performed first with hydrogen-nitrogen and then with xenon-hydrogen. In a few cases, due to small variations in the water content of the samples, a second hydrogen-nitrogen diffusion test has also been undertaken. The mean experimental xenon and hydrogen diffusion coefficients obtained from the tests are given in Table (4). Between 3 and 6 measures were made to obtain each value, except for the 3% RH which is based on a single measure. Theoretical estimates of the xenon diffusion coefficient in cement paste in case of predominant ordinary or Knudsen diffusion are also given in Table (4), based respectively on Eqs. (16) or (17) and on the mean hydrogen diffusion coefficients obtained during the tests.

The evolution with RH of the xenon diffusion coefficient in the CEM I cement paste is presented graphically in Figure (7), together with that of the hydrogen diffusion coefficient and the theoretical estimates in case of predominant Knudsen or ordinary diffusion mechanisms. Figure (7) shows that the shape of the curves obtained for xenon and hydrogen are very similar. First, they decrease slowly till 70% RH and then sharply. The measured diffusion coefficients for xenon are overall 5 to 20 times smaller than that of hydrogen. In the tests performed on saturated samples (100% HR), no xenon flow has been observed, even after a year. It appears therefore that

the diffusion of xenon in cement paste becomes very difficult when the percentage of unsaturated pores tends towards zero.

The 3% RH measure apart, the xenon to hydrogen diffusion coefficients ratio is almost constant in the RH range 55-82%, with a mean value of 0.1, close to the theoretical estimate of Eq. (17) in the case of Knudsen diffusion (0.124). This means that the unsaturated porous space available to gas diffusion at RHs less than or equal to 82% is fully accessible to hydrogen and xenon. This is not the case when the RH is greater or equal to 93% since the xenon to hydrogen diffusion coefficients ratio drops respectively to 0.05 and 0 for RHs of 93 and 100%.

These results can possibly be attributed to the formation of discontinuities in the porous network accessible to gas diffusion. When pore humidity is high, the narrow connections (necks) that exist between large pores which are still unsaturated can be filled with liquid water [5]. Hence, the diffusion of a gas through nearly saturated materials depends on the solubility and on the diffusion coefficient of the gas in the liquid phase that saturates the pore necks. The solubility of xenon in water is five times greater than that of hydrogen and cannot therefore explain the lack of xenon diffusion through the nearly saturated CEM I cement paste samples. Its important size (the atomic radius of xenon is almost six times greater than that of hydrogen), which would limit its diffusion in saturated narrow pore connections, could however be at the origin of these results.

4.4. Impact of the total gas pressure on gas diffusion

The total gas pressure dependency is one of the major difference that exists between ordinary and Knudsen diffusion in porous media. In case of ordinary diffusion, the diffusion coefficient of a gas species in a porous medium is inversely proportional to the total pressure, see Eqs. (4) and (5). In case of Knudsen diffusion, it does not depend on the total pressure of the gas phase, see Eqs. (7) and (8). To determine which is the dominant diffusion mechanism in cementitious materials, hydrogen diffusion tests have been performed at four different pressures (0.1, 0.5, 1 and 1.9 bars) on samples of the two CEM I cement pastes in equilibrium with air at 3, 55, 70 and 82% RH. One sample per RH and cement paste type has been tested at the four different pressures in a random order.

The hydrogen diffusion coefficients measured at the four different pressures and on the different cement pastes are given in Table (5). As shown by these results, whatever the RH and the cement paste, the hydrogen diffusion coefficient decreases with increasing pressure. This trend is consistent qualitatively with an ordinary diffusion mechanism. However, quantitatively, the evolution of the hydrogen diffusion coefficient is far from being proportional to $1/P$. This can be best seen by plotting the $D_i(P)/D_i(1 \text{ bar})$ diffusion coefficient ratio in function of the pressure ratio $1/P$ (bar/bar), as illustrated in Figure (8). In case of a purely ordinary diffusion mechanism, $D_i(P)/D_i(P_o) = P_o/P$, as shown by the continuous line in Figure (8). In case of a purely Knudsen diffusion mechanism, $D_i(P)/D_i(P_o) = 1$, as indicated by the dashed line in Figure (8).

Figure (8) shows that all the test results (circles and triangles) are close to the pure Knudsen diffusion mechanism line, indicating that the total pressure of the gas phase has little impact on the hydrogen diffusion coefficient in cement paste. Obviously, the pressure dependency of the diffusion mechanism at hand in cement paste does not vary with the hygral state of the cement paste, i.e., its internal RH. This means that it is the same diffusion mechanism which dominates in cement paste when the capillary pores and/or the micropores are accessible to the gas phase. The complex pore connections and tortuosity in cement paste are very probably at the origin of this result. In fact, the diffusion path through cementitious materials can be seen as a succession of meso- and micropores connected by necks which makes therefore the overall gas flow dependent on the size of the smallest pores. In the studied pressure range 0.1-1.9 bars, the dominant diffusion mechanism is therefore of Knudsen type and reflects the importance of the interactions between the gas molecules and the pore structure of the material.

5. Conclusions

In this paper, experimental results on gas diffusion in three cement pastes have been presented. The main conclusions of this study are :

1. Gas diffusion depends essentially on the saturation level of the cement paste (which determines the percentage of pores available to gas), and hence on the RH of air when the material is in equilibrium with its external environment. The hydrogen diffusion coefficient was found to vary between 10^{-6} m²/s for dry samples and 10^{-13}

m^2/s for saturated samples.

2. The total porosity and the pore size distribution/connectivity of cement paste have a strong impact on hydrogen diffusion. Capillary pores are of great importance with regards to gas diffusion in cementitious materials since the diffusion coefficient decreases strongly in the RH range 55-100%. On the contrary, as shown by the lack of variation of diffusion properties when the RH is smaller than 55%, micropores play a negligible role with regards to gas diffusion in cementitious materials.

3. Gas diffusion in CEM I cement paste depends approximately on the square root of the gas molecular weight, except when the saturation level of the material is high, i.e., when the RH is greater or equal to 93%. This limit is probably due to the discontinuity of the unsaturated pore network at high RH which makes gas diffusion through nearly saturated cementitious materials dependent on the gas solubility and gas diffusion properties in liquid water.

4. In the pressure range 0.1 – 1.9 bars, gas diffusion in CEM I cement paste depends slightly on the total pressure of the gas phase. This result indicates that Knudsen diffusion mechanisms are dominant in these materials. The pore size (capillary pores or micropores) and the saturation level have no impact on this tendency. These results need to be confirmed for higher total gas pressures.

References

- [1] Saetta A.V., Schrefler B.A., Vitaliani R.V., The carbonation of concrete and the mechanism of moisture, heat and carbon dioxide flow through porous materials, *Cem Conc Res*, 23, 761-772, 1993.
- [2] Chaussadent T., *State of the art and considerations about the carbonation of reinforced concrete*, [In French], Etudes et Recherches des Laboratoire des Ponts et Chaussées, OA29, Paris, 1999.
- [3] Bary B., Sellier A., Coupled moisture-carbon dioxide-calcium transfer model for carbonation of concrete, *Cem Conc Res*, 34, 1859-1872, 2004.
- [4] Daian J.-F., *Transport in porous media*, 3, 563-589, 1988.
- [5] Xi Y., Bazant Z.P., Molina L., Jennings H.M., Moisture diffusion in cementitious materials, *Advn Cem Bas Mat*, 1, 258-266, 1994.
- [6] Mainguy M., Coussy O., Eymard R., *Modelling of isothermal hydric transfers in porous media. Application to the drying of cement-based materials*, [In French], Etudes et Recherches des Laboratoire des Ponts et Chaussées, OA32, Paris, 1999.
- [7] Mason E.A., Malinauskas A.P., *Gas transport in porous media : the dusty-gas model*, Elsevier, Amsterdam, 1983.
- [8] Kobayashi K., Shuttoh K., Oxygen diffusivity of various cementitious materials, *Cem and Conc Res*, 21, 273-284, 1991.

- [9] Ohama Y., Demura K., Kobayashi K., Satoh Y., Morikawa M., Pore size distribution and oxygen diffusion resistance of polymer-modified mortars, *Cem and Conc Res*, 21, 309-315, 1991.
- [10] Sharif A., Loughlin K.F., Azad A.K., Navaz C.M., Determination of the effective diffusion coefficient in concrete via a gas diffusion technique, *ACI Mat Journ*, 94, 3, 227-233, 1997.
- [11] Klink T., Gaber K., Schlattner E., Setzer M.J., Characterization of the gas transport properties of porous materials by determining the radon diffusion coefficient, *Materials and Structures*, 32, 749-754, 1999.
- [12] Reinecke S.A., Sleep B.E., Knudsen diffusion, gas permeability, and water content in an unconsolidated porous medium, *Water Resources Research*, Vol. 38, No. 12, 16.1-16.15, 2002.
- [13] Carman P.C., *Flow of gases through porous media*, Butterworths Scientific Publications, London, 1956.
- [14] Millington R.J., Gas diffusion in porous media, *Science*, 130, 100-102, 1959.
- [15] Klinkenberg L.J. The permeability of porous media to liquids and gases, *API Drilling and producing Practices*, 1941, 200-213.
- [16] Reid R.C., Prausnitz J.M., Sherwood T.K., *The properties of gases and liquids*, Third Ed., McGraw-Hill, New York, 1977.

- [17] Gosse J., Transport properties of gases at moderate pressures, [In French], In Les Techniques de l'Ingénieur, Constantes Physico-Chimiques, K 425, 2005.
- [18] Powers T.C., Brownyard T.L. Studies of the physical properties of hardened Portland cement paste, *Journal of the American Concrete Institute*, 1947, **9**, No. 22, 971-992.
- [19] Baroghel-Bouny V. *Characterization of cement pastes and concretes : methods, analysis, interpretations*, [In French], Doctoral dissertation, *Laboratoire Central des Ponts et Chaussées* [In French], 1994, Paris.
- [20] Gallé C., Daian J.-F., Gas permeability of unsaturated cement-based materials: application of a multi-scale network model, *Mag Conc Res*, 52 (4), 251-263, 2000.
- [21] Gallé C., Effect of drying on cement-based materials pore structure as identified by mercury intrusion porosimetry. A comparative study between oven-, vacuum-, and freeze-drying, *Cem and Conc Res*, 31, 1467-1477, 2001.
- [22] Richet C. Migration of radioelements within cementitious materials. Impact of leaching on transport mechanism, [In French], *Doctoral thesis*, University of Paris XI, 1992.
- [23] Taylor H.F.W. *Cement chemistry, 2nd Edition*, Thomas Telford, London, 1997.

Appendix

The data used in this paper to calculate the xenon-nitrogen and hydrogen-nitrogen free diffusion coefficients are summarized in Table (6).

The characteristic length σ_{12} of Eq. (4) has been estimated as follows :

$$\sigma_{12} = \frac{1}{2}(\sigma_1 + \sigma_2) \quad (18)$$

[17] gives the following approximate expression to determine the diffusion collision integral Ω_D :

$$\begin{aligned} \Omega_D = & 1.06036 \times (T^*)^{-0.1561} + 0.193 \times EXP[-0.47635T^*] \\ & + 1.03587 \times EXP[-1.52996T^*] + 1.76474 \times EXP[-3.89411T^*] \end{aligned} \quad (19)$$

with

$$T^* = \frac{kT}{\epsilon_{12}} \quad (20)$$

and

$$\frac{\epsilon_{12}}{k} = \left[\left(\frac{\epsilon_1}{k} \right) \left(\frac{\epsilon_2}{k} \right) \right]^{1/2} \quad (21)$$

List of Tables

Table 1 : Salt solutions and related Relative Humidities

Table 2: Properties of the tested cement paste materials

Table 3: Mean hydrogen diffusion coefficients (m^2/s) obtained on the CEM I and CEM V cement paste samples (total pressure 1 bar).

Table 4: Mean xenon and hydrogen diffusion coefficients (m^2/s) obtained on the CEM I w/c 0.45 cement paste samples and theoretical estimates of the xenon diffusion coefficient in case of predominant ordinary (Eq. 16) or Knudsen (Eq. 17) diffusion mechanisms.

Table 5: Hydrogen diffusion coefficients (m^2/s) obtained on the CEM I and CEM V cement paste samples tested at 0.1, 0.5, 1 and 1.9 bars

Table 6: Parameters used in Eq. (4) to calculate the free diffusion coefficients of hydrogen and xenon in nitrogen.

List of Figures

Figure 1: Transport processes in porous media

Figure 2: Sketch of the diffusion cell

Figure 3: Sketch of the experimental set-up used for the diffusion tests.

Figure 4: Estimation of the Knudsen-ordinary diffusion coefficient from experimental results.

Figure 5: Effective diffusion coefficients versus RH for the CEM I cement paste samples (w/c ratios of 0.35 and 0.45).

Figure 6: Effective diffusion coefficients versus RH for the CEM I and CEM V cement paste samples with a w/c ratio of 0.45.

Figure 7: Hydrogen and Xenon effective diffusion coefficients versus RH for the CEM I cement paste samples with a w/c ratio of 0.45.

Figure 8: Hydrogen diffusion coefficients ratio versus total pressure ratio for the tests performed on CEM I and CEM V cement paste samples at 0.1, 0.5, 1 and 1.9 bars.

Table 1: Salt solutions and related Relative Humidities

RH (T=20°C)	54.5%	69.9%	81.8%	93.2%	100%
Salt solution	Mg(NO ₃) ₂ ,H ₂ O	KI	KBr	KNO ₃	H ₂ O

Table 2: Properties of the tested cement paste materials

Cement type	CEM I	CEM I	CEM V
w/c ratio	0.35	0.45	0.45
wet density (g/cm ³)	2.08	2.0	1.92
porosity (water)	27%	34%	35%

Table 3: Mean hydrogen diffusion coefficients (m^2/s) obtained on the CEM I and CEM V cement paste samples (total pressure 1 bar).

HR (%)	3	55	70	82	93
CEM I w/c 0.35	$8.6 \cdot 10^{-7}$	$7.8 \cdot 10^{-7}$	$3.8 \cdot 10^{-8}$	$6.1 \cdot 10^{-11}$	$8.4 \cdot 10^{-11}$
CEM I w/c 0.45	$1.4 \cdot 10^{-6}$	$1.6 \cdot 10^{-6}$	$5.8 \cdot 10^{-7}$	$3.5 \cdot 10^{-10}$	$1.3 \cdot 10^{-10}$
CEM V w/c 0.45	$7.5 \cdot 10^{-8}$	$3.0 \cdot 10^{-8}$	$5.0 \cdot 10^{-9}$	$4.5 \cdot 10^{-9}$	$2.1 \cdot 10^{-12}$

Table 4: Mean xenon and hydrogen diffusion coefficients (m^2/s) obtained on the CEM I w/c 0.45 cement paste samples and theoretical estimates of the xenon diffusion coefficient in case of predominant ordinary (Eq. 16) or Knudsen (Eq. 17) diffusion mechanisms.

HR (%)	3	55	70	82	93
Hydrogen	$1.3 \cdot 10^{-6}$	$1.9 \cdot 10^{-6}$	$6.6 \cdot 10^{-7}$	$4.5 \cdot 10^{-10}$	$1.3 \cdot 10^{-10}$
Xenon	$3.0 \cdot 10^{-7}$	$1.9 \cdot 10^{-7}$	$5.5 \cdot 10^{-8}$	$6.3 \cdot 10^{-11}$	$7.1 \cdot 10^{-12}$
Xenon Eq. (16)	$2.2 \cdot 10^{-7}$	$3.2 \cdot 10^{-7}$	$1.1 \cdot 10^{-7}$	$7.4 \cdot 10^{-11}$	$2.2 \cdot 10^{-11}$
Xenon Eq. (17)	$1.7 \cdot 10^{-7}$	$2.4 \cdot 10^{-7}$	$8.1 \cdot 10^{-8}$	$5.6 \cdot 10^{-11}$	$1.7 \cdot 10^{-11}$

Table 5: Hydrogen diffusion coefficients (m^2/s) obtained on the CEM I cement paste samples tested at 0.1, 0.5, 1 and 1.9 bars

Pressure (bars)	0.1	0.5	1	1.9
CEM I w/c 0.35 HR 3%	$2.01 \cdot 10^{-6}$	$1.27 \cdot 10^{-6}$	$1.05 \cdot 10^{-6}$	$8.04 \cdot 10^{-7}$
CEM I w/c 0.35 HR 55%	$1.72 \cdot 10^{-6}$	$1.41 \cdot 10^{-6}$	$1.18 \cdot 10^{-6}$	$9.07 \cdot 10^{-7}$
CEM I w/c 0.35 HR 70%	$7.4 \cdot 10^{-8}$	$7.24 \cdot 10^{-8}$	$5.45 \cdot 10^{-8}$	$4.47 \cdot 10^{-8}$
CEM I w/c 0.35 HR 82%	$2.28 \cdot 10^{-10}$	$1.79 \cdot 10^{-10}$	$1.15 \cdot 10^{-10}$	$7.98 \cdot 10^{-11}$
CEM I w/c 0.45 HR 3%	$2.31 \cdot 10^{-6}$	$1.39 \cdot 10^{-6}$	$1.08 \cdot 10^{-6}$	$1.09 \cdot 10^{-6}$
CEM I w/c 0.45 HR 55%	$3.27 \cdot 10^{-6}$	$2.95 \cdot 10^{-6}$	$2.45 \cdot 10^{-6}$	$1.81 \cdot 10^{-6}$
CEM I w/c 0.45 HR 70%	$1.14 \cdot 10^{-6}$	$9.93 \cdot 10^{-7}$	$8.02 \cdot 10^{-7}$	$6.21 \cdot 10^{-7}$
CEM I w/c 0.45 HR 82%	$3.64 \cdot 10^{-9}$	$3.52 \cdot 10^{-9}$	$2.69 \cdot 10^{-9}$	$2.70 \cdot 10^{-9}$

Table 6: Parameters used in Eq. (4) to calculate the free diffusion coefficients of hydrogen and xenon in nitrogen.

	M_i (g/mol)	σ_i (Å)	ϵ_i/k (K)
H ₂	2.016	2.827	59.7
N ₂	28.0	3.568	113.0
Xe	131.3	4.061	225.3

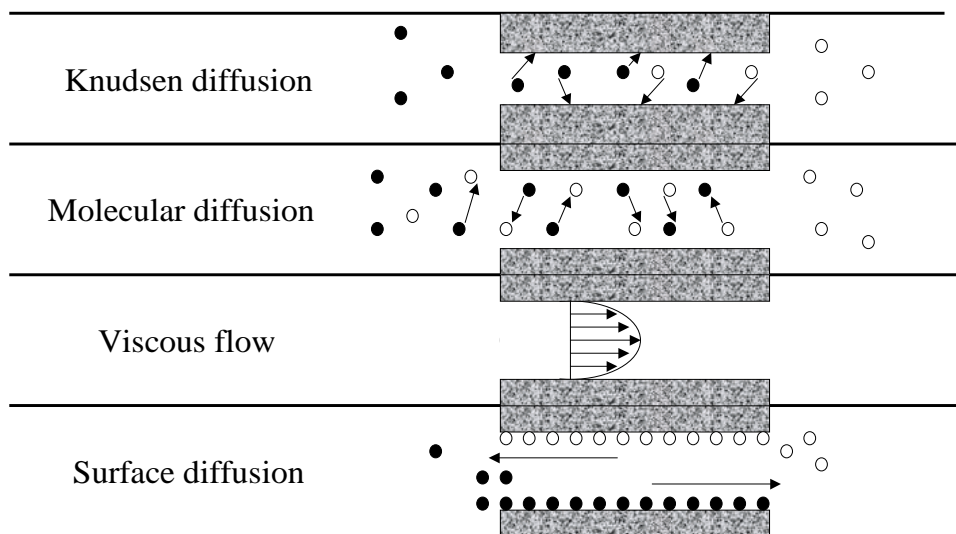


Figure 1: Transport processes in porous media

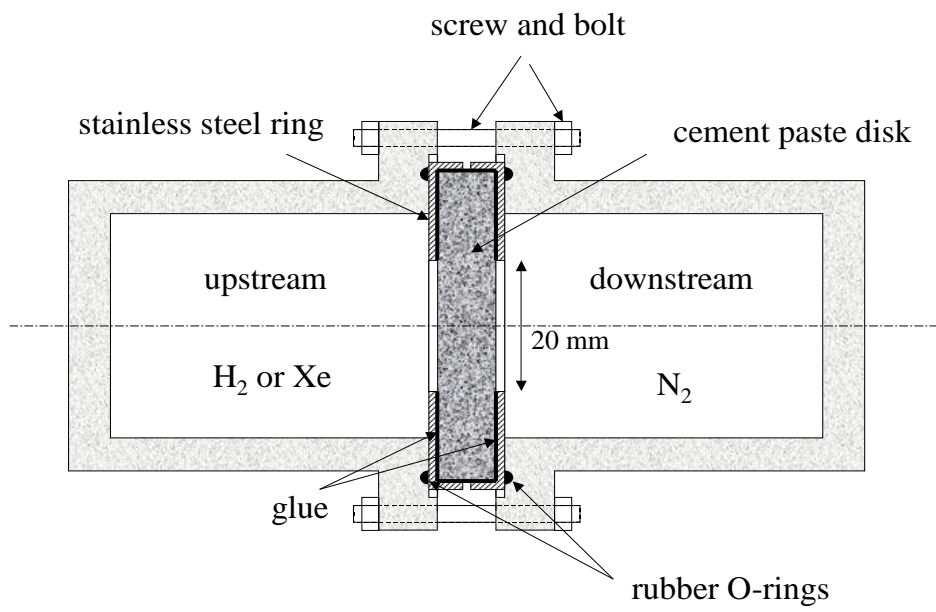


Figure 2: Sketch of the diffusion cell

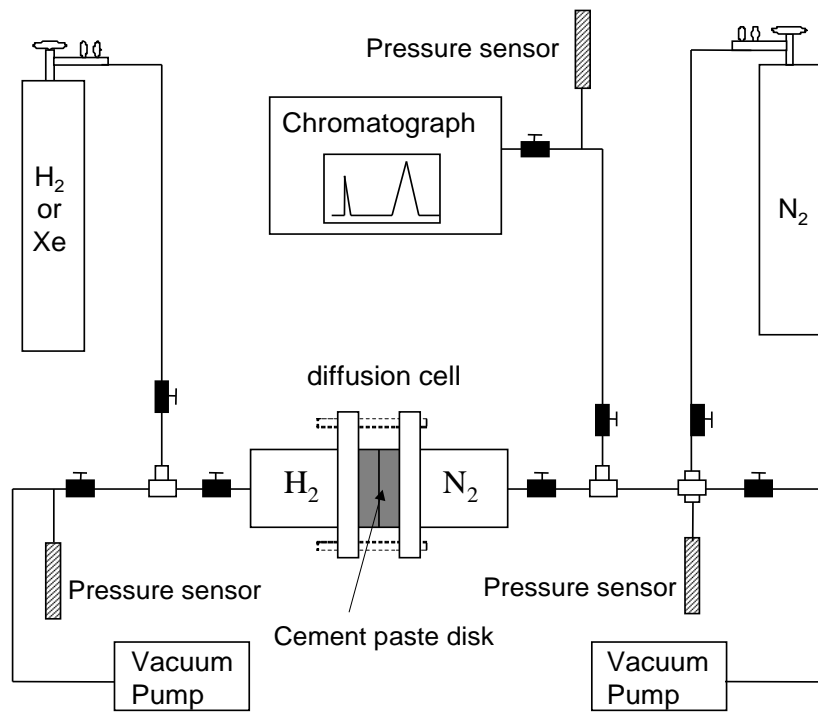


Figure 3: Sketch of the experimental set-up used for the diffusion tests.

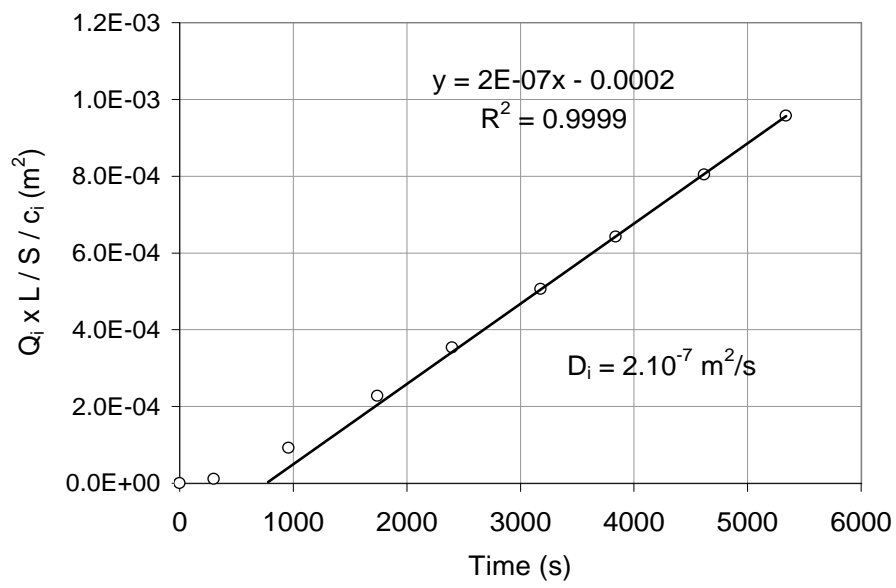


Figure 4: Estimation of the diffusion coefficient from experimental results.

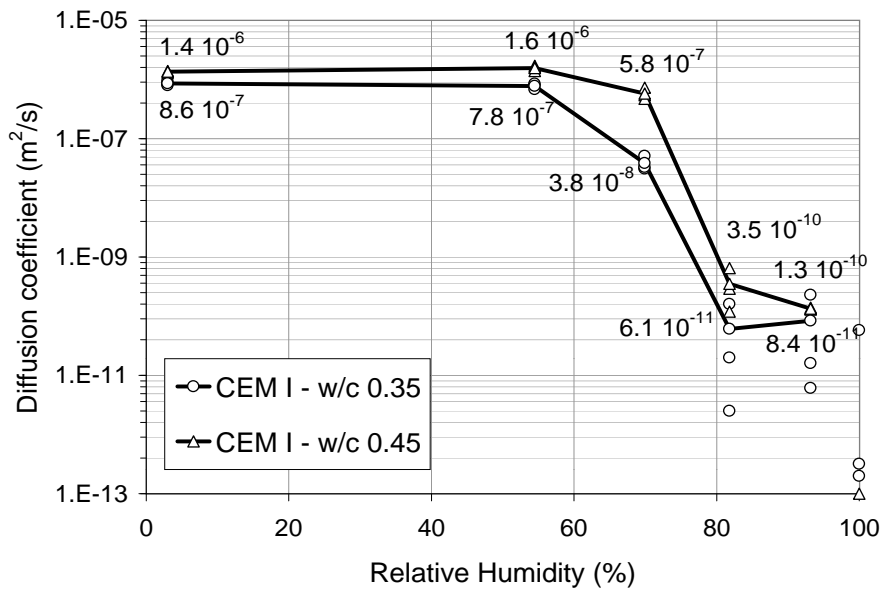


Figure 5: Hydrogen diffusion coefficients versus RH for the CEM I cement paste samples (w/c ratios of 0.35 and 0.45).

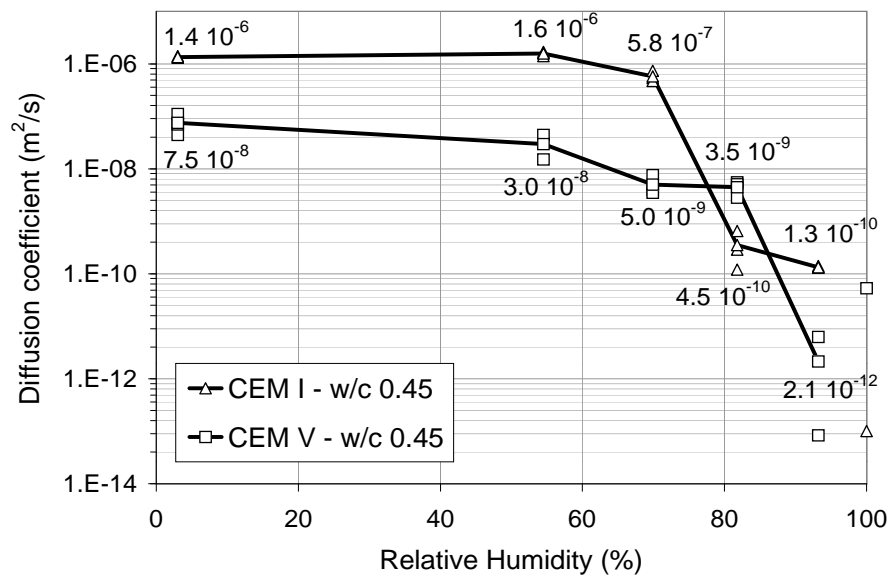


Figure 6: Hydrogen diffusion coefficients versus RH for the CEM I and CEM V cement paste samples with a w/c ratio of 0.45.

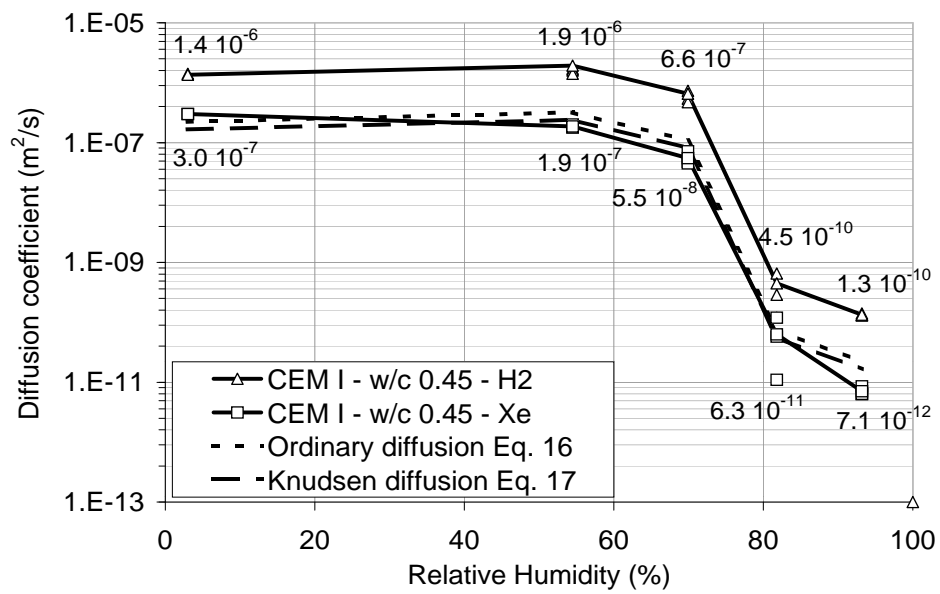


Figure 7: Hydrogen and Xenon diffusion coefficients versus RH for the CEM I cement paste samples with a w/c ratio of 0.45.

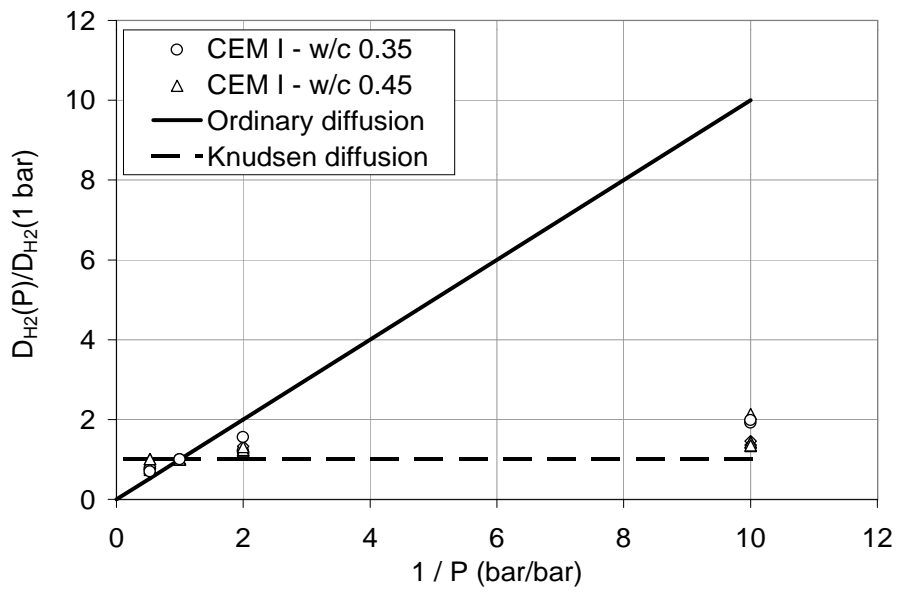


Figure 8: Hydrogen diffusion coefficients ratio versus total pressure ratio for the tests performed on CEM I and CEM V cement paste samples at 0.1, 0.5, 1 and 1.9 bars